Journal of Molecular and Cellular Cardiology 82 (2015) 174–183

Contents lists available at ScienceDirect

Journal of Molecular and Cellular Cardiology

journal homepage: www.elsevier.com/locate/yjmcc

Original article

Experimental heart failure modelled by the cardiomyocyte-specific loss of an epigenome modifier, DNMT3B☆

A. Vujic [a,b], E.L. Robinson [a], M. Ito [c], S. Haider [d], M. Ackers-Johnson [a,b,e], K. See [e], C. Methner [f], N. Figg [a], P. Brien [g], H.L. Roderick [g], J. Skepper [c], A.Ferguson-Smith [c], R.S. Foo [a,b,e,*]

[a] Division of Cardiovascular Medicine, Addenbrooke's Centre for Clinical Investigation Building, University of Cambridge, Cambridge CB2 0QQ, UK
[b] Cardiovascular Research Institute, Centre for Translational Medicine MD6, National University Health System, 117599 Singapore
[c] Department of Physiology, Development and Neuroscience, University of Cambridge, Cambridge CB2 3EG, UK
[d] Centre for Molecular Oncology, Barts Cancer Institute, London EC1M 6BQ, UK
[e] Genome Institute of Singapore, 60 Biopolis Street, 138672 Singapore
[f] Clinical Pharmacology Unit, Addenbrooke's Centre for Clinical Investigation Building, University of Cambridge, Cambridge CB2 0QQ, UK
[g] Epigenetics ISP, Babraham Institute, Cambridge CB22 3AT, UK

ARTICLE INFO

Article history:
Received 8 October 2014
Received in revised form 6 March 2015
Accepted 9 March 2015
Available online 14 March 2015

Keywords:
Epigenome
DNA methylation
Heart failure
Alternative splicing

ABSTRACT

Differential DNA methylation exists in the epigenome of end-stage failing human hearts but whether it contributes to disease progression is presently unknown. Here, we report that cardiac specific deletion of *Dnmt3b*, the predominant DNA methyltransferase in adult mouse hearts, leads to an accelerated progression to severe systolic insufficiency and myocardial thinning without a preceding hypertrophic response. This was accompanied by widespread myocardial interstitial fibrosis and myo-sarcomeric disarray. By targeted candidate gene quantitative RT-PCR, we discovered an over-activity of cryptic splice sites in the sarcomeric gene *Myh7*, resulting in a transcript with 8 exons missing. Moreover, a region of differential methylation overlies the splice site locus in the hearts of the cardiac-specific conditional knockout (CKO) mice. Although abundant and complex forms of alternative splice variants have been reported in diseased hearts and the contribution of each remains to be understood in further detail, our results demonstrate for the first time that a link may exist between alternative splicing and the cardiac epigenome. In particular, this gives the novel evidence whereby the loss of an epigenome modifier promotes the development and progression of heart disease.

© 2015 Elsevier Ltd. All rights reserved.

1. Introduction

Despite remarkable improvements in medical therapy, the prognosis of patients with cardiac failure remains poor, with almost 50% of patients dying within 5 year of initial diagnosis. The incidence and prevalence of cardiac failure is on the rise rapidly worldwide [1]. Thus, new therapeutic approaches are urgently needed. Cardiac failure develops often after a prolonged asymptomatic phase, accompanied by changes in heart mass, size and shape, a process known as pathological remodelling [2,3]. It is attributed in some cases to a complex genetic predisposition and/or multiple environmental factors [4]. Nonetheless, gene expression changes are often consistent in a failing heart, regardless of the original inciting cause. Therefore, it would be important to explore whether regulating gene expression in heart failure could be a therapeutic approach. One mechanism of gene expression regulation that has gained importance is epigenetics. The epigenome, unlike the genome, undergoes dynamic changes throughout the course of life. The epigenome, modifiable by diet and environment, may hence contribute to and maintain adaptive and deviant gene expression states [5,6]. Globally, the patterns of DNA methylation established by de novo DNA methyltransferases DNMT3a and DNMT3b during embryogenesis are maintained by DNMT1 and remain stable throughout development and adulthood. However, age, sex and environmental cardiovascular risk factors have been associated with specific alteration of DNA methylation at individual loci [7–9]. Genome-wide profiling of DNA methylation in blood from participants in the Normative Aging study showed that lower LINE-1 methylation in peripheral blood leukocytes is a predictor of incidence and mortality from ischemic heart disease and stroke [10]. Experimental animal models have demonstrated that DNA methylation plays a critical role in the development of atherosclerosis and cardiovascular disease [8]. In humans, *DNMT3B* mutations are causing the rare autosomal recessive disorder *I*mmunodeficiency, *C*entromeric instability and *F*acial anomalies (ICF) Syndrome, associated with severe mental retardation disorders and immunodeficiency [11]. Characterization of the heart has not

☆ One sentence summary: Loss of DNA methyltransferase 3B leads to progressive heart failure.

* Corresponding author at: Cardiovascular Research Institute, Centre for Translational Medicine MD6, National University Health System, 117599 Singapore.
E-mail address: mdcrfsy@nus.edu.sg (R.S. Foo).

http://dx.doi.org/10.1016/j.yjmcc.2015.03.007
0022-2828/© 2015 Elsevier Ltd. All rights reserved.

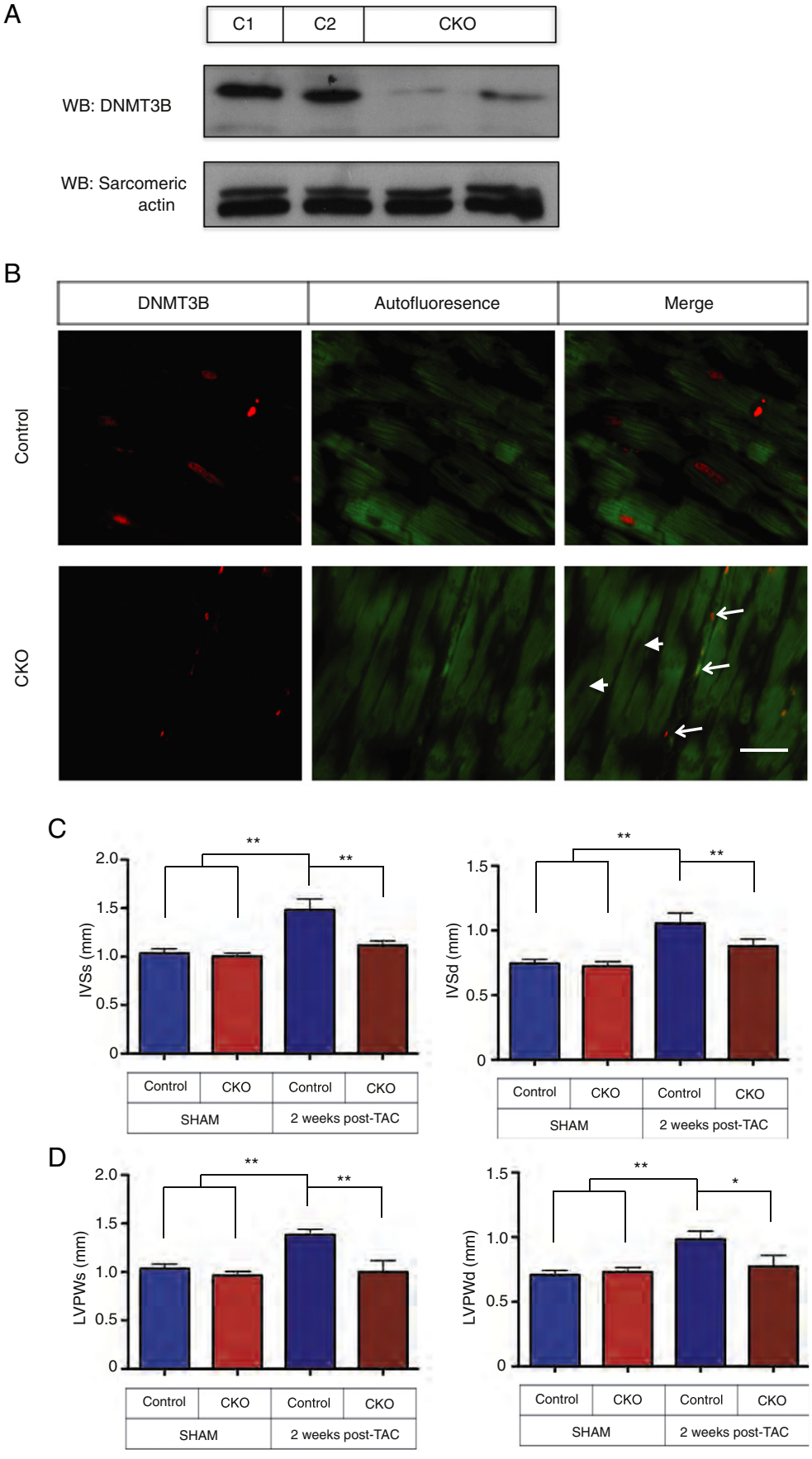
A
C1
C2
CKO
WB: DNMT3B
WB: Sarcomeric actin
B
DNMT3B
Autofluoresence
Merge
Control
CKO
C
IVSs (mm)
IVSd (mm)
2.0
1.5
1.0
0.5
0
**
**
Control
CKO
Control
CKO
SHAM
2 weeks post-TAC
D
LVPWs (mm)
LVPWd (mm)
**
**
*

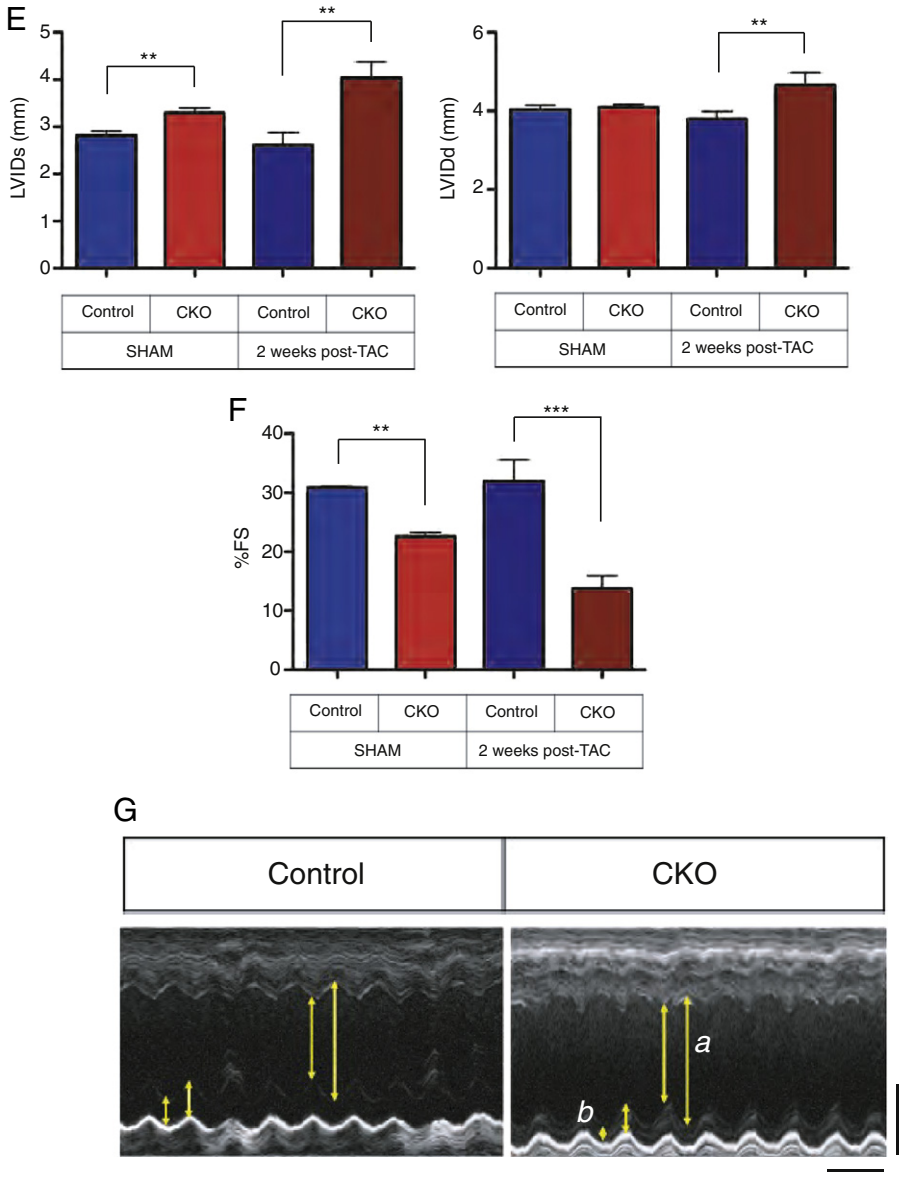

Fig. 1. Cardiac-specific loss of DNMT3B predisposes to cardiomyopathy. (A), Western blotting for DNMT3B with mouse whole LV from tamoxifen(tam)-treated *Dnmt3b*$^{+/+}$; *MerCreMer*$^{+}$ (called "C1"), vehicle-treated *Dnmt3b*$^{2lox/2lox}$; *MerCreMer*$^{+}$ (called "C2"), and tam-treated *Dnmt3b*$^{2lox/2lox}$, *MerCreMer*$^{+}$ (called "CKO"). Sarcomeric actin was used to show equal protein loading. (B), Immunofluorescent histochemistry showed DNMT3B staining (red) in the nuclei of Control hearts; whereas in CKO hearts, loss of staining was specifically in cardiomyocytes (arrowheads), but not in the nuclei of non-cardiomyocytes (arrows). Autofluorescence (green) enabled cardiomyocytes to be recognised by the visualisation of myofibrils. Bar represents 10 μm. Echocardiographic measurement of (C) interventricular septal and (D) posterior wall dimensions in end-systole and end-diastole (IVSs, IVSd, PWs and PWd respectively) showed that 2 weeks following transverse aortic constriction (TAC), Control hearts mounted the expected hypertrophic response but this was significantly blunted in CKO hearts. Similarly, 2 weeks post-TAC Control hearts showed compensated and sustained (E) LV internal dimensions in end-systole and end-diastole (LVIDs and LVIDd), and (F) fractional shortening (%FS), whereas post-TAC CKO hearts showed direct transition to decompensated contractile function with significant increase in LVIDs and LVIDd, and decrease in %FS. Notably, CKO hearts at 2 weeks following Sham surgery alone showed detectable deterioration in systolic function (LVIDs and %FS). Echocardiography was performed with at least N = 10 in each group. Statistical analysis was performed using Students *t*-test. $^{*}p < 0.05$, $^{**}p < 0.01$, $^{***}p < 0.001$. (G), Echocardiography was performed 8 weeks after tam treatment (without TAC) in CKO. M-mode scan showed distinctive features of LV chamber enlargement (arrows a) and thinning of posterior wall (arrows b) in CKO. Scale: 200 ms and 2 mm. Quantitative dimensions of hearts 8-weeks post-tam (CKO compared to C1 and C2 control hearts) are displayed in Table 1.

been possible in all cases because of premature death. However interestingly, *Dnmt3b* knockout mice die between E13.5 and E16.5 with cardiac ventricular septal defects amongst others, suggesting that DNMT3b is necessary for cardiac ventricular septum development and function [12]. We previously found that the epigenome of end-stage failing human hearts differ from that of healthy normal controls [13,14]. This dysregulation of DNA methylation may alter the expression of genes related to increased disease susceptibility. We therefore set out to examine whether perturbation to the epigenome contributes to heart failure development and progression.

2. Results

2.1. DNA methyltransferase 3b,(DNMT3b) is the predominant DNA methyltransferase in the heart

To verify cardiac expression of DNMT3b we used a panel of protein lysates; mouse tissues, human cell lines and normal human heart. We determined that the main DNA methyltransferase expressed in human and mouse hearts is DNMT3B, whereas the other methyltransferases, DNMT1 and DNMT3A were virtually undetectable (Supplementary

Table 1
Echocardiograhic and LV catheterisation parameters of hearts from Control and CKO mice. C1: *Dnmt3b*$^{+/+}$, *MerCreMer*$^{+}$ (tam-treated); C2: *Dnmt3b*$^{2lox/2lox}$, *MerCreMer*$^{+}$ (vehicle-treated); CKO: *Dnmt3b*$^{2lox/2lox}$, *MerCreMer*$^{+}$ (tam-treated). Echo and LV catheterisation were performed 8 weeks after administration of Tam or vehicle.

	C1	C2	CKO
LVIDd (mm)	4.25 ± .11	4.19 ± .08	4.05 ± .07
LVIDs (mm)	2.88 ± .09	2.91 ± .06	3.20 ± .06**
IVSd (mm)	0.89 ± .06	0.85 ± .02	0.85 ± .03
IVSs (mm)	1.35 ± .07	1.23 ± .04	1.22 ± .04
PWd (mm)	0.80 ± .03	0.75 ± .03	0.77 ± .03
PWs (mm)	1.20 ± .03	1.16 ± .03	1.00 ± .02*
%FS	32.21 ± .99	30.39 ± .97	22.50 ± .76**
HR (beats/min)	527.7 ± 66.4	564.1 ± 53.7	464.7 ± 73
BW (g)	29.3 ± .67	27.9 ± .55	29.2 ± .66
HW (mg)	140.3 ± 4.4	134.7 ± 4.0	138.0 ± 3.1
HW/BW	5.14 ± .13	4.83 ± .14	4.73 ± .07
HW/TL	7.04 ± .17	6.40 ± .22	6.48 ± .14
+ dP/dT (mm Hg/s)	9026.3 ± 543.4	8516.6 ± 333.2	3897.3 ± 519.6*
+ dP/dT with dobutamine (mm Hg/s)	10931.5 ± 397.2	11246.2 ± 318.5	6411.9 ± 935.0*
− dP/dT (− mm Hg/s)	7929.6 ± 601.1	7329.5 ± 741.4	6155.7 ± 562.7
− dP/dT with dobutamine (− mm Hg/s)	8500.7 ± 557.9	8511.8 ± 300.0	3195.5 ± 440.6

Figs. S1, S2). We therefore proceeded to generate an inducible cardiac-specific *Dnmt3b* knockout mouse to explore whether loss of this methyltransferase specifically in cardiomyocytes, affects cardiac function.

2.2. Cardiac specific Dnmt3b deletion induced compromised systolic function in vivo

First, we crossed mice bearing the *Dnmt3b*$^{2lox/2lox}$ alleles [15] with transgenic mice that express Cre recombinase in a tamoxifen(tam)-inducible and cardiomyocyte-specific manner, *αMHC-MerCreMer* [16]. We employed 2 sets of control mice *Dnmt3b*$^{+/+}$, *MerCreMer*$^{+}$ (tam-treated) (we called "C1") and *Dnmt3b*$^{2lox/2lox}$, *MerCreMer*$^{+}$ (vehicle-treated) (we called "C2"), and the conditional knockout mouse *Dnmt3b*$^{2lox/2lox}$, *MerCreMer*$^{+}$ (tam-treated) (we called "CKO"). Tam administered over 4 days in 8-week-old adult CKO mice induced approximately 70% reduction in DNMT3B protein levels by week-1 post-tam (Fig. 1A), but no detectable change in DNMT1 or 3A (Supplementary Fig. S3). Loss of DNMT3B specifically and only in cardiomyocytes was also confirmed by immunohisto-chemistry (Fig. 1B). Both sets of control mice showed normal and indistinguishable cardiac function on echocardiography. *Dnmt3b*$^{2lox/2lox}$, *MerCreMer*$^{+}$ (vehicle-treated) mice ("C2") were therefore used as control for subsequent experiments unless otherwise indicated. We saw no effects of the *Dnmt3b* deletion on basal LV function at the immediate stage upon cre-recombinase activation by tam. We therefore proceeded to subject CKO mice week-1 post-tam and control mice to myocardial stress by thoracic transverse aortic constriction (TAC). Control mice responded to TAC with the expected robust level of hypertrophy by 2-weeks post-TAC, with thickened interventricular septal and left ventricular posterior wall dimensions in both systole and diastole (IVSs, IVSd and LVPWs, LVPWd respectively) (Figs. 1C, D), with compensated and sustained contractile function as demonstrated by unchanged chamber dimensions (LVIDs and LVIDd) and fractional shortening (%FS) (Figs. 1E, F). Conversely, CKO mice showed a blunted hypertrophic response (Figs. 1C, D) that was accompanied by a significant increase in LV chamber size and fall in %FS (Figs. 1E, F), indicative of severely decompensated contractile function. The same was seen in mice treated with systemic administration of isoprenaline by infusion pump (Supplementary Table 1), reflecting the consistent outcome of blunted hypertrophic response and accelerated progression to decompensation resulting from cardiomyocyte loss of DNMT3b regardless of the form of myocardial stress.

Simultaneously, we made the unexpected observation that even CKO mice that had undergone sham surgery, spontaneously developed a detectable fall in %FS with an increase in LVIDs but only after a longer period post-Tamoxifen induction (i.e. 3–4 weeks following cre-recombinase activation) (comparison between sham:control and sham:CKO in Fig. 1F), suggesting that sustained loss of DNMT3B could itself be leading to compromised systolic function. We therefore followed up un-operated CKO mice over a longer time course and confirmed that 8 weeks following tam-induction alone (without surgery), CKO mice, but not either set of Control mice, developed significantly reduced %FS, increased LVIDs and decreased LVPWs (Table 1), reflecting that this progression to significant systolic insufficiency was related to DNMT3b-loss itself. Pressure measurements from LV catheterisation also corresponded with compromised systolic function in these mice (Table 1). Both sets of control mice (C1 and C2, as described above) were used in order to confidently implicate DNMT3b-loss for the progression to systolic insufficiency.

2.3. Dnmt3b knockout hearts had widespread interstitial fibrosis and myo-sarcomeric disarray

To explore the mechanism leading to contractile dysfunction in CKO hearts, we examined LV sections from CKO hearts by histology. In keeping with the lack of echocardiographic evidence of hypertrophy, cardiomyocytes from CKO hearts had unchanged cell widths (Supplementary Fig. S4). A potential explanatory for myocardial thinning is an increase in cell death. Therefore to assess if DNMT3B deletion led to any significant cell loss, we performed TUNEL staining on heart sections. Exceedingly low levels of TUNEL positive cells were identified in CKO hearts (<3 per mm^3) and even so, these were only identified in non-cardiomyocytes (Fig. S5). No evidence of cardiomyocyte cell death was detected. Instead widespread interstitial fibrosis was obvious on Masson's trichrome staining (Fig. 2A) and marked myo-sarcomeric disarray was evident on electron-micrography (Fig. 2B and Supplementary Fig. S6).

Foetal gene expression changes are a paradigm for myocardial stress especially in the context of myocardial hypertrophy. However, in striking similarity to the lack of a hypertrophic response in CKO compared to WT-TAC hearts (Supplementary Fig. S4), there were also no significant changes in foetal gene expression by the same comparisons (Supplementary Fig. S7). On the other hand, we reasoned that in order to explain the contractile dysfunction in CKO hearts and based on foregoing histological findings, loss of DNMT3B may lead to altered expression of pro-fibrogenic or sarcomeric genes. TGF-β signalling has been implicated in fibroblast activation and myocardial fibrosis [17,18]. We therefore examined CKO hearts by quantitative RT-PCR prior to the onset of interstitial fibrosis (before week-8), but did not find any differential expression of genes in the TGF-β signalling pathway (not shown). This contradicted the possibility that the primary defect in CKO hearts is mediated by an early TGF-β dependent mechanism. We further checked transcript abundance of various sarcomeric genes including *Mybpc3*, *Tnnt2* and *Tnni3*, and similarly did not find any overall differential expression of these genes (not shown). Instead we noticed on quantitative RT-PCR of *Myh7* that amplicons targeting specifically only certain exons of the *Myh7* gene showed differential transcript levels between CKO and control hearts.

2.4. Sarcomeric gene Myh7 was alternatively spliced in the CKO

We examined *Myh7* transcripts more closely and discovered an over-activity of cryptic splice sites within exons 13, 26 and 28 in CKO hearts (Figs. 3A, B). Complex alternative splicing of *MYH7* has been described in human cardiomyopathy [19]. We looked but did not find any differential levels in splicing variants of other sarcomeric genes (*Myh6*, *Mybpc3*, *Tnnt2* and *Tnni3*), and hence focussed our attention on *Myh7*.

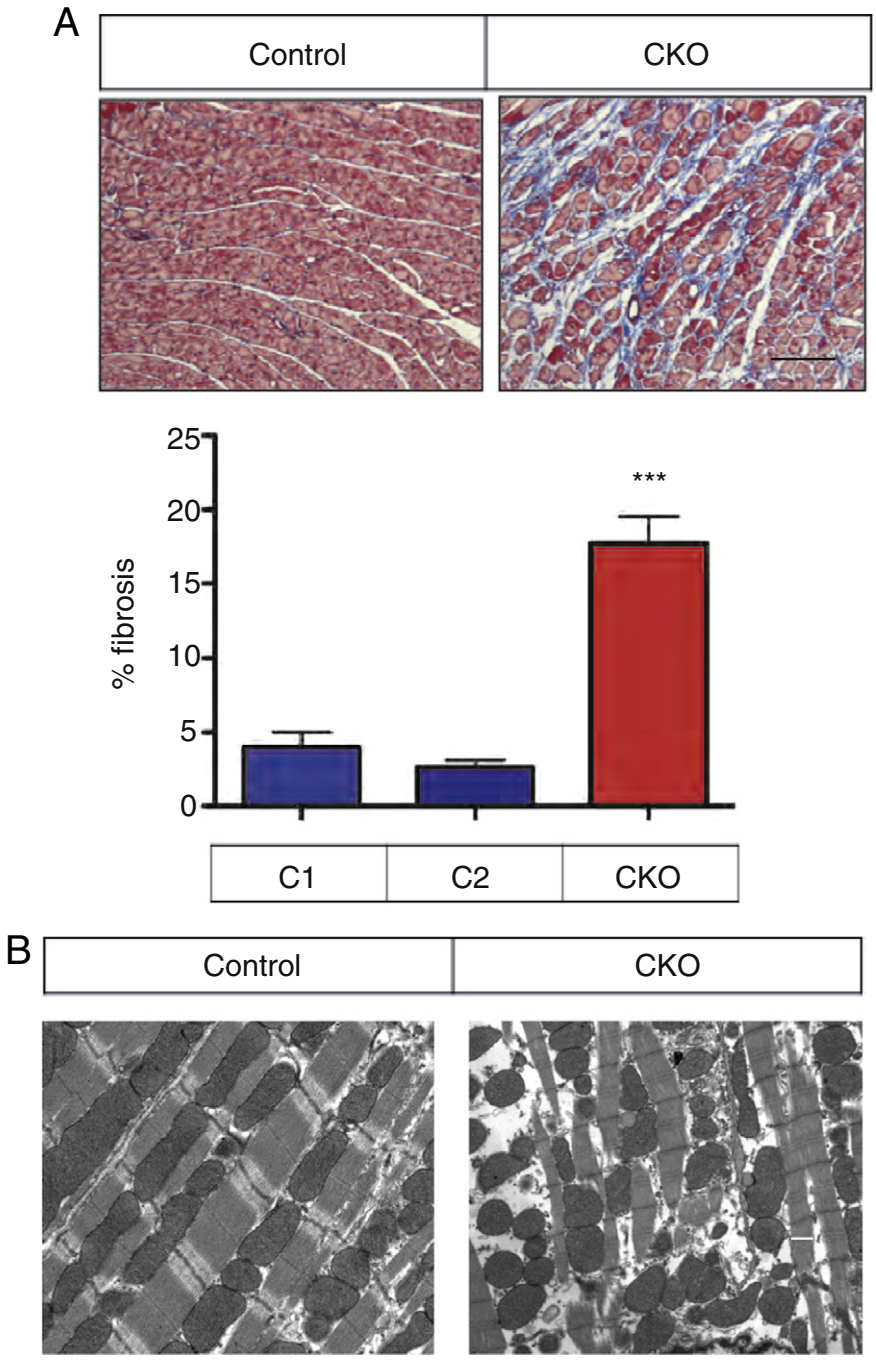

Fig. 2. (A), Masson's trichrome staining showed significant and widespread interstitial fibrosis (blue) which was quantified as %area of each histological section. Black bar represents 100 μm. Three sections were examined for each of 5 hearts in each group. Students *t*-test, *** $p < 0.001$. (B), Electron micrographs of cardiomyocyte nuclei in CKO hearts showed significant myo-sarcomeric disarray. White bars represent 500 nm. Supplementary Fig. S6 shows further examples of electron micrographs.

Fig. 3. CKO hearts showed increased levels of *Myh7* alternative splicing. (A), shows the exon-intron structure of *Myh7* from exon 13 to exon 29, and novel cryptic splice sites. White boxes indicate exons missing in the alternatively spliced transcript (AST). Orange boxes indicate stretches of intronic sequence that are incorporated into the AST. Arrows indicate positions of Forward (F) and Reverse (R) primers used to amplify the cryptic splice sites in (B). (B), Cryptic splice sites were amplified using primer pairs F13-R28 and F26-R28. F28-R29 was used as a positive control primer pair. PCR products were visualised on a 2% agarose gel and showed that cryptic spliced junctions could be amplified in all hearts but more abundantly in CKO. Negative control "minus RT" showed an absence of PCR products. (C), PCR products from (B) were sequenced, aligned to the mouse reference genome and proven to be novel cryptic splice sites. (D), Shows the positions of primer-probe pairs used for quantitative RT-PCR for amplicons 1 to 4. Sequences of primers and probes are listed in Supplementary Tables 2 and 3. (E–H), Relative quantities of amplicons 1 to 4 were normalised to total *Myh7* transcripts. Total *Myh7* transcript abundance did not differ between groups (not shown). PCR were performed in triplicate and at least N = 8 were used for each group. Statistical analysis was performed by Students *t*-test, ** $p < 0.01$, *** $p < 0.001$. (I), Immunofluorescent histochemistry using anti-MYH7 antibody labelled perinuclear aggregates (arrows) that co-localised with Ubiquitin in CKO, but not Control hearts. Bar represents 10 μm. See Supplementary Fig. S10 for further examples. (J), Vertical bars across the exon–intron structure of *Myh7* indicates individual CpGs. %Methylation for each CpG within clusters 1 to 4 was measured by pyrosequencing using gDNA from Control (blue) and CKO (red) hearts. Sequencing was performed in 5 technical replicates and at least N = 5 hearts were used in each group. Statistical analysis was performed by Students *t*-test. * $p < 0.05$, ** $p < 0.01$.

In CKO hearts, we performed strand-specific RT-PCR for *Myh7* and PCR products containing the cryptic splice junctions were verified by sequencing (Figs. 3B, C). Next, we designed specific primer-probe sets for RT-PCR to quantify the abundance of either alternative spliced transcript (AST) only (Fig. 3D, amplicons 1, 2), wild type *Myh7* transcript only (amplicon 3), or both transcripts (amplicon 4), and verified that AST were significantly more abundant in CKO hearts compared to controls (Figs. 3E–F). Conversely wild-type transcripts were significantly reduced in CKO, and total *Myh7* transcripts unchanged (Figs. 3G, H), indicating a preferential switch towards the usage of

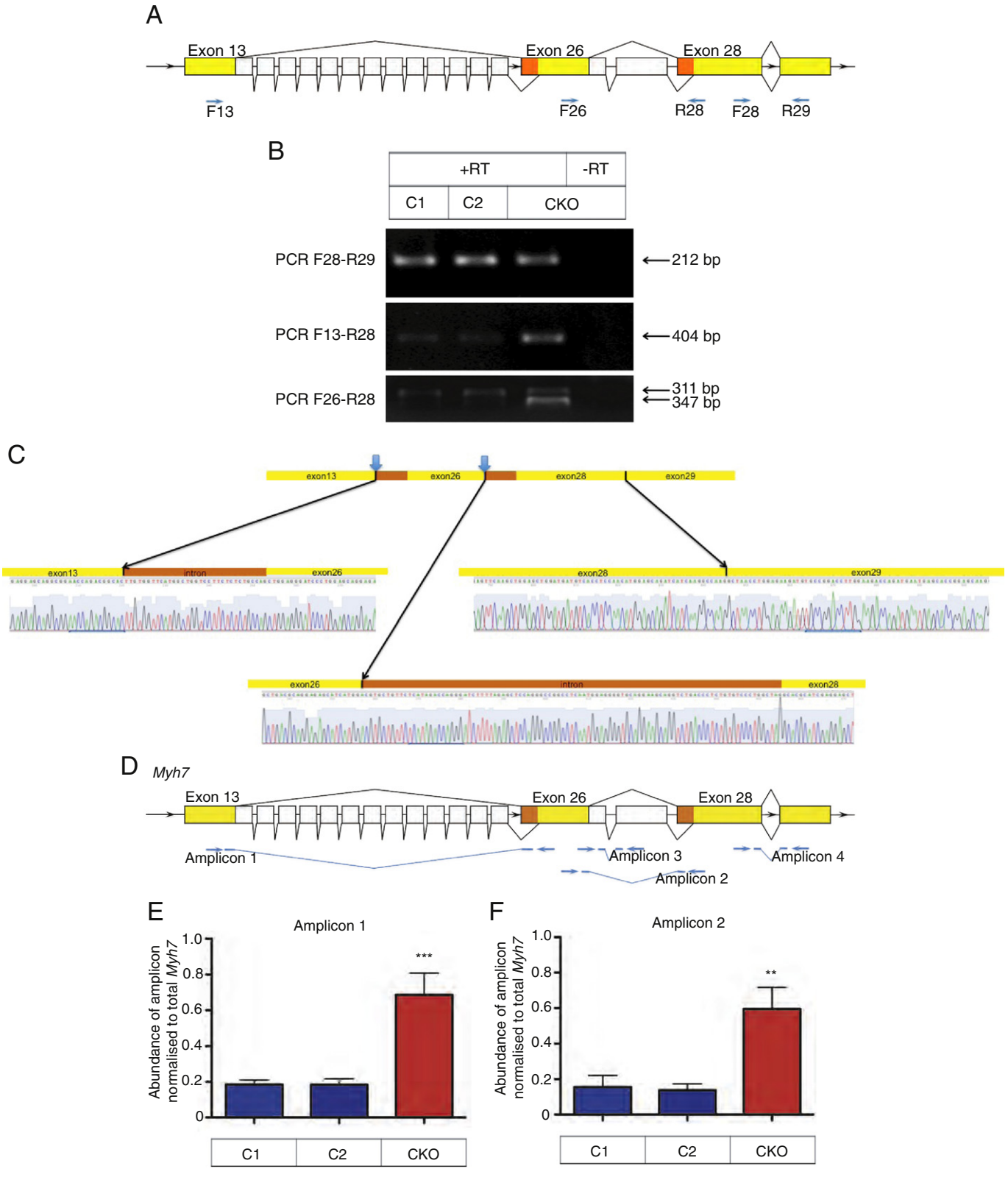

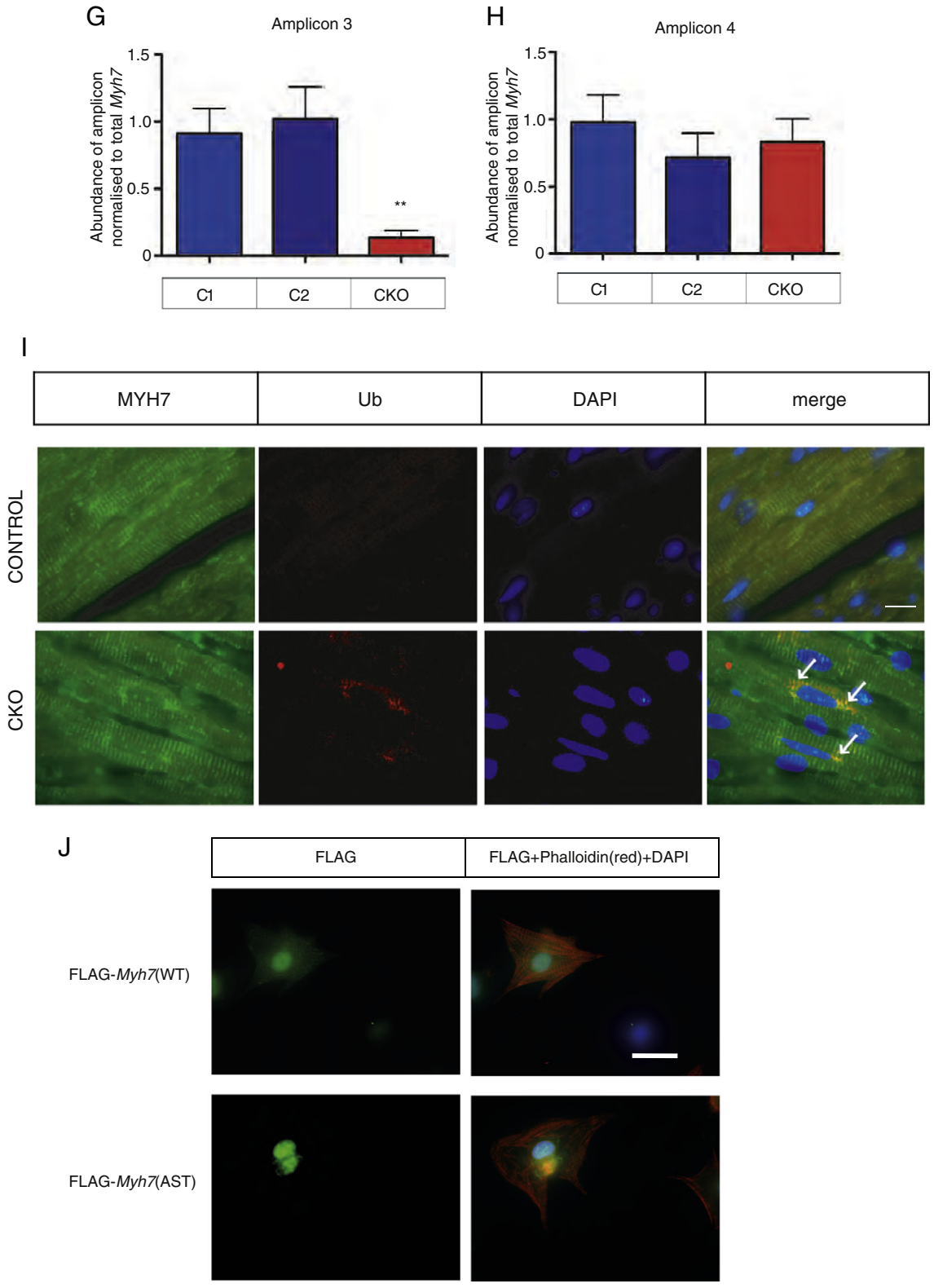

Fig. 3 (*continued*).

the cryptic splice sites in CKO hearts. We returned to CKO hearts that underwent surgical TAC and verified that the abundance of AST was again substantially higher in CKO hearts that underwent TAC, than control (Supplementary Fig. S8). More notably, control hearts that underwent TAC did not show significant increase in AST in relation to wild-type *Myh7* transcripts, indicating that myocardial stress alone was not sufficient to switch usage to these cryptic splice sites, and also implying that AST and the switch to cryptic splice usage is not merely secondary to myocardial stress but a result of the loss of DNMT3B.

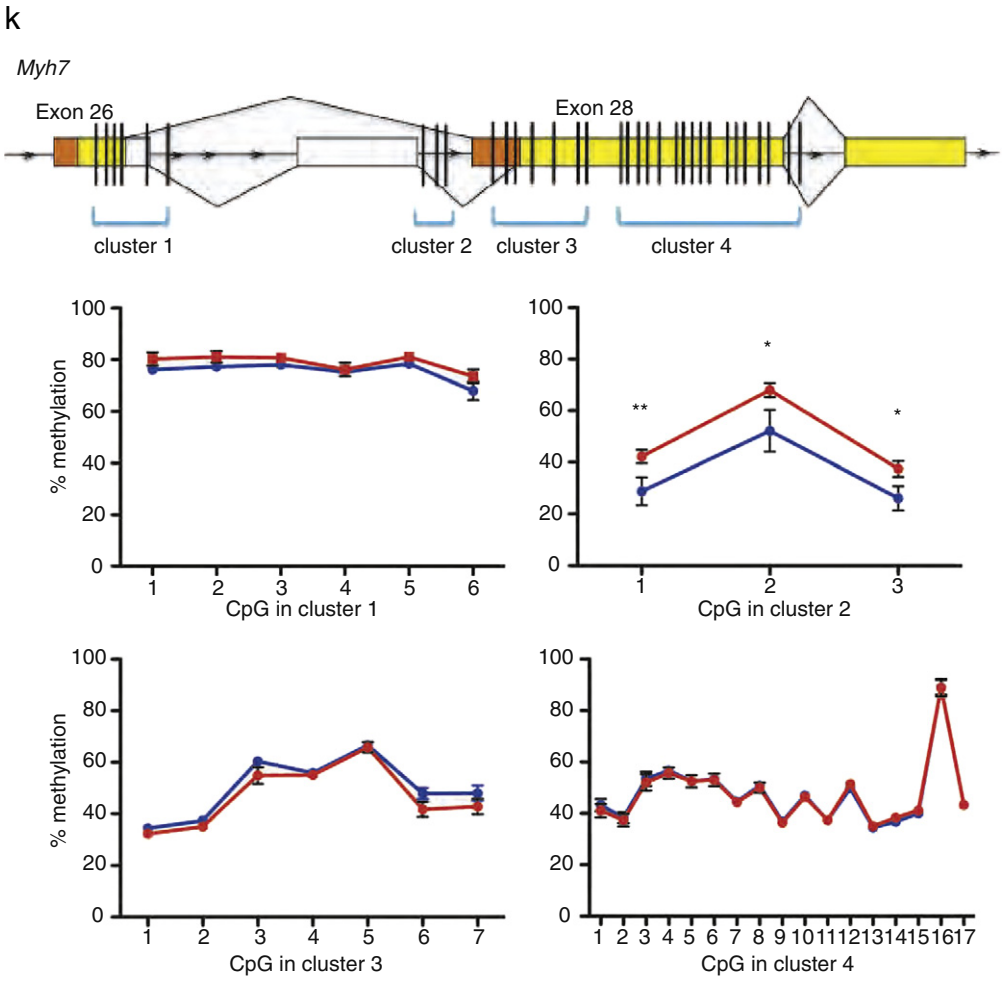

Fig. 3 (*continued*).

2.5. Alternatively spliced Myh7 formed perinuclear aggregates marked ubiquitin-related degradation

Alignment of the AST predicts that it lacks 8 exons and generates a premature termination codon. Quantifiable abundance of AST in CKO hearts however suggests that to some extent, some of this transcript escaped nonsense mediated decay. Indeed, if translated, the AST may encode a 47 kDa peptide missing many key C-terminal domains of MYH7. We therefore probed whole cardiac protein lysates from CKO and control hearts using an anti-MYH7 antibody, and found that there were additional immunoreactive bands in the Western blot for CKO hearts corresponding to the ~40–50 kDa molecular weight (Supplementary Fig. S9). Interestingly, anti-MYH7 antibody also labelled perinuclear aggregates that co-localised with ubiquitin (Fig. 3I, and Supplementary Fig. S10), suggesting that CKO hearts may contain MYH7 immunoreactive proteins that were targeted for ubiquitin-related degradation.

Accumulation of aggregates may represent defective and ubiquitin-labelled proteins that are resistant to degradation in CKO or that emerging cardiomyopathy itself resulted in inefficient processing of protein degradation. To test the in vitro expression of AST in cardiomyocytes, we generated both wild-type and AST FLAG-tagged constructs of *Myh7* (FLAG-*Myh7*-WT and FLAG-*Myh7*-AST) (Supplementary Fig. S11). Unlike FLAG-MYH7-WT that followed an expected sarcomeric distribution when overexpressed in neonatal rat cardiomyocytes, FLAG-MYH7-AST formed perinuclear aggregates (Fig. 3J, and Supplementary Fig. S12), consistent with our observation in CKO-hearts. Overexpression of either construct did not lead to differential levels of cardiomyocyte apoptosis (not shown). We could not explain immunoreactivity of our FLAG antibody observed in the nucleus, but this may imply sarcomeric protein presence in the nucleus as observed previously for troponin [31], and here made more prominent by overexpression. Nuclear immunoreactivity was consistent with both FLAG-*Myh7*-WT and FLAG-*Myh7*-AST constructs, but the striking difference remained that AST resulted in perinuclear aggregates, compared to a sarcomeric distribution of the WT construct.

Mechanisms of alternative splicing in the heart have previously implicated the role of specific splicing factors (ASF/SF2 and CUGBP1) [20–22]. We checked but did not find any difference in the protein abundance of these splicing factors in CKO hearts (Supplementary Fig. S11).

2.6. Differential methylation overlays the alternatively spliced Myh7 transcript

Finally we assessed the effect of DNMT3B loss on the DNA methylation profile at the *Myh7* locus in CKO and control hearts. We inspected the *Myh7* genomic sequence and noticed that a CpG-rich locus overlies the site of alternative splicing. We proceeded to assay for differential DNA methylation of each of the series of cytosine nucleotides within this locus by pyrosequencing. Remarkably, contrary to the exact same methylation profiles between control and CKO in other cystosines at the locus, methylation of 3 cytosines (CpGs) within intron 27 were significantly different (Fig. 3K).

3. Discussion

Epigenetic modifications, such as DNA methylation and histone modifications, represent attractive disease mechanisms because they might help to explain how environmental and lifestyle factors can impose aberrant gene expression patterns in an individual's lifetime that can result in increased cardiovascular risk. Herein we report that deletion of a de novo DNA methyltransferase, DNMT3B, in the adult mouse heart correlated with alternative splicing of the important sarcomeric gene *Myh7*, myosarcomeric disarray and an onset of cardiomyopathy. The loss or inactivation of DNMT3B may not directly represent disease mechanism in human heart failure, but we have utilised this model as proof of concept that loss of the de novo methyltransferase resulted in methylation change in at least one cardiac-relevant locus which we have tested. Indeed in our hands, DNMT3B protein levels were not significantly altered in human cardiomyopathic hearts compared to healthy control (data not shown). Hence, instead we have utilised this experimental mouse model to demonstrate that perturbation of DNA methyltransferase in the heart led to accelerated heart failure. Specifically, our data correlates a change in the epigenome overlying an over-activity of cryptic splice sites within *Myh7*, in CKO hearts, and an accumulation of alternatively spliced transcripts and possible truncated protein products in the heart with emergent contractile insufficiency. The latter fits well with existing data showing that other chromatin structures such as histone modification [23] and DNA factor binding-mediated pausing of RNA polymerase II [24] regulate alternative splicing in other specific contexts. This study implies that, as in neurons that are the other archetypal non-dividing cells, dynamic methylation states may also exist in terminally differentiated adult cardiomyocytes. Crystal co-structure analysis of DNMT1 with oligonucleotides containing CpGs suggests that unmethylated CpGs are not accessible to the DNMT1 active site unless CpGs are hemimethylated [25]. For non-dividing cells that undergo dynamic turnover of methylation and de-methylation, without prior requirement for hemi-methylated CpGs, the DNMT3A and DNMT3B are therefore likely to be the crucial DNA methyltransferases. The increase in DNA methylation observed at the cryptic splice sites within *Myh7*, in CKO is surprising given that patients with loss of *DNMT3b* activity exhibit hypomethylation of pericentromeric regions and selective demethylation of promoters associated with altered gene expression [26]. Since DNMT3A was not upregulated upon *DNMT3b* deletion it likely that there is another mechanism that induces locus specific methylation increase following the loss of DNMT3B. In concordance with our previous studies that showed that end-stage cardiomyopathic human hearts have significantly more hypomethylated CGIs and gene promoters than healthy control hearts [14], this data supports that a re-distribution in methylation patterns, rather than a loss of global methylation is the difference between a healthy and cardiomyopathic heart, even if the initiating cause is loss of a DNA methyltransferase. The mechanism for locus-specific increased methylation will require further elucidation. Significant evidence has suggested a close relation between pathophysiology of heart failure and increased oxidative stress and DNA damage [27–29]. The precise contribution of alternatively spliced transcripts to heart disease progression is likely to be context-specific, and although diseased hearts are now known to have a significant, varied and complex accumulation of alternatively spliced transcripts, the contribution of each to disease progression will need further study [19,30]. Our results here however provide the first hint that RNA splicing in the heart can be affected by the epigenome. If the cardiac epigenome is dynamic and subject to external factors, it could potentially have a far-reaching role in cardiac failure disease development and progression.

4. Methods

See supplementary materials.

Disclosures

None to declare.

Acknowledgements

This work was supported by a Wellcome Trust (086796/Z/08/Z) PhD studentship to A.V. and a British Heart Foundation Project Grant (PG12/2008). Further support was also from the National Medical Research Council of Singapore (NMRC/CSA/046/2012).

Appendix A. Supplementary data

Supplementary data to this article can be found online at http://dx.doi.org/10.1016/j.yjmcc.2015.03.007.

References

[1] American Heart Association. Heart disease and stroke statistics—2003 update. Dallas, Tex: American Heart Association; 2002.
[2] Hill JA, Olson EN. Cardiac plasticity. N Engl J Med 2008;358(13):1370–80.
[3] Hill JA, Olson EN. Muscle: fundamental biology and mechanisms of disease. New York, NY: Academic Press; 2012.
[4] McNally EM, Golbus JR, Puckelwartz MJ. Genetic mutations and mechanisms in dilated cardiomyopathy. J Clin Invest 2013;123(1):19–26.
[5] Baccarelli A, Rienstra M, Benjamin EJ. Cardiovascular epigenetics: basic concepts and results from animal and human studies. Circ Cardiovasc Genet 2010;3(6):567–73.
[6] Suzuki MM, Bird A. DNA methylation landscapes: provocative insights from epigenomics. Nat Rev Genet 2008;9(6):465–76.
[7] Bjornsson HT, Sigurdsson MI, Fallin MD, Irizarry RA, Aspelund T, Cui H, et al. Intra-individual change over time in DNA methylation with familial clustering. JAMA 2008;299(24):2877–83.
[8] Turunen MP, Aavik E, Yla-Herttuala S. Epigenetics and atherosclerosis. Biochim Biophys Acta 2009;1790(9):886–91.
[9] Zaina S, Lindholm MW, Lund G. Nutrition and aberrant DNA methylation patterns in atherosclerosis: more than just hyperhomocysteinemia? J Nutr 2005;135(1):5–8.
[10] Bollati V, Schwartz J, Wright R, Litonjua A, Tarantini L, Suh H, et al. Decline in genomic DNA methylation through aging in a cohort of elderly subjects. Mech Ageing Dev 2009;130(4):234–9.
[11] Lana E, Megarbane A, Tourriere H, Sarda P, Lefranc G, Claustres M, et al. DNA replication is altered in Immunodeficiency Centromeric instability Facial anomalies (ICF) cells carrying DNMT3B mutations. Eur J Hum Genet 2012;20(10):1044–50.
[12] Okano M, Bell DW, Haber DA, Li E. DNA methyltransferases Dnmt3a and Dnmt3b are essential for de novo methylation and mammalian development. Cell 1999;99(3):247–57.
[13] Haider S, Cordeddu L, Robinson E, Movassagh M, Siggens L, Vujic A, et al. The landscape of DNA repeat elements in human heart failure. Genome Biol 2012;13(10):R90.
[14] Movassagh M, Choy MK, Knowles DA, Cordeddu L, Haider S, Down T, et al. Distinct epigenomic features in end-stage failing human hearts. Circulation 2011;124(22):2411–22.
[15] Lin H, Yamada Y, Nguyen S, Linhart H, Jackson-Grusby L, Meissner A, et al. Suppression of intestinal neoplasia by deletion of Dnmt3b. Mol Cell Biol 2006;26(8):2976–83.
[16] Sohal DS, Nghiem M, Crackower MA, Witt SA, Kimball TR, Tymitz KM, et al. Temporally regulated and tissue-specific gene manipulations in the adult and embryonic heart using a tamoxifen-inducible Cre protein. Circ Res 2001;89(1):20–5.
[17] Teekakirikul P, Eminaga S, Toka O, Alcalai R, Wang L, Wakimoto H, et al. Cardiac fibrosis in mice with hypertrophic cardiomyopathy is mediated by non-myocyte proliferation and requires Tgf-beta. J Clin Invest 2010;120(10):3520–9.
[18] Koitabashi N, Danner T, Zaiman AL, Pinto YM, Rowell J, Mankowski J, et al. Pivotal role of cardiomyocyte TGF-beta signaling in the murine pathological response to sustained pressure overload. J Clin Invest 2011;121(6):2301–12.
[19] Kong SW, Hu YW, Ho JW, Ikeda S, Polster S, John R, et al. Heart failure-associated changes in RNA splicing of sarcomere genes. Circ Cardiovasc Genet 2010;3(2):138–46.
[20] Kalsotra A, Xiao X, Ward AJ, Castle JC, Johnson JM, Burge CB, et al. A postnatal switch of CELF and MBNL proteins reprograms alternative splicing in the developing heart. Proc Natl Acad Sci U S A 2008;105(51):20333–8.
[21] Kalsotra A, Wang K, Li PF, Cooper TA. MicroRNAs coordinate an alternative splicing network during mouse postnatal heart development. Genes Dev 2010;24(7):653–8.
[22] Xu X, Yang D, Ding JH, Wang W, Chu PH, Dalton ND, et al. ASF/SF2-regulated CaMKIIdelta alternative splicing temporally reprograms excitation–contraction coupling in cardiac muscle. Cell 2005;120(1):59–72.
[23] Luco RF, Pan Q, Tominaga K, Blencowe BJ, Pereira-Smith OM, T, Misteli. Regulation of alternative splicing by histone modifications Science 2010;327(5968):996–1000.
[24] Shukla S, Kavak E, Gregory M, Imashimizu M, Shutinoski D, Kashlev M, et al. CTCF-promoted RNA polymerase II pausing links DNA methylation to splicing. Nature 2011;479(7371):74–9.
[25] Hermann A, Goyal R, Jeltsch A. The Dnmt1 DNA-(cytosine-C5)-methyltransferase methylates DNA processively with high preference for hemimethylated target sites. J Biol Chem 2004;279(46):48350–9.

[26] Brun ME, Lana E, Rivals I, Lefranc G, Sarda P, Claustres M, et al. Heterochromatic genes undergo epigenetic changes and escape silencing in immunodeficiency, centromeric instability, facial anomalies (ICF) syndrome. PLoS One 2011;6(4):e19464.
[27] Kameda K, Matsunaga T, Abe N, Hanada H, Ishizaka H, Ono H, et al. Correlation of oxidative stress with activity of matrix metalloproteinase in patients with coronary artery disease. Possible role for left ventricular remodelling. Eur Heart J 2003;24(24):2180–5.
[28] Siggens L, Figg N, Bennett M, Foo R. Nutrient deprivation regulates DNA damage repair in cardiomyocytes via loss of the base-excision repair enzyme OGG1. FASEB J 2012;26(5):2117–24.
[29] Li JM, Gall NP, Grieve DJ, Chen M, Shah AM. Activation of NADPH oxidase during progression of cardiac hypertrophy to failure. Hypertension 2002;40(4):477–84.
[30] Lee JH, Gao C, Peng G, Greer C, Ren S, Wang Y, Xiao X. Analysis of transcriptome complexity through RNA sequencing in normal and failing murine hearts. Circ Res 2001; 109(12):1332–41.
[31] Bergmann O, Bhardwaj RD, Bernard S, Zdunek S, Barnabe-Heider F, Walsh S, et al. Evidence for cardiomyocyte renewal in humans. Science 2009;324(5923):98–102.